Thirty years of satellite-derived lava discharge rates at Etna: Implications for steady volumetric output

Andrew J.L. J.L. Harris, Andrea Steffke, Sonia Calvari, Letizia Spampinato

Thirty years of satellite-derived lava discharge rates at Etna: Implications for steady volumetric output

Andrew Harris,[1] Andrea Steffke,[2] Sonia Calvari,[3] and Letizia Spampinato[3]

Received 18 January 2011; revised 22 April 2011; accepted 10 May 2011; published 9 August 2011.

[1] We present a 30 year long data set of satellite-derived time-averaged lava discharge rates (TADR) for Mount Etna volcano (Sicily, Italy), spanning 1980–2010 and comprising 1792 measurements during 23 eruptions. We use this to classify eruptions on the basis of magnitude and intensity, as well as the shape of the TADR time series which characterizes each effusive event. We find that while 1983–1993 was characterized by less frequent but longer-duration effusive eruptions at lower TADRs, 2000–2010 was characterized by more frequent eruptions of shorter duration and higher TADRs. However, roughly the same lava volume was erupted during both of these 11 year long periods, so that the volumetric output was linear over the entire 30 year period, increasing at a rate of 0.8 m^3 s^{-1} between 1980 and 2010. The cumulative volume record can be extended back in time using data available in the literature. This allows us to assess Etna's output history over 5 centuries and to place the current trend in historical context. We find that output has been stable at this rate since 1971. At this time, the output rate changed from a low discharge rate phase, which had characterized the period 1759 to 1970, to a high discharge rate phase. This new phase had the same output rate as the high discharge rate phase that characterized the period 1610–1669. The 1610–1669 phase ended with the most voluminous eruption of historic times.

Citation: Harris, A., A. Steffke, S. Calvari, and L. Spampinato (2011), Thirty years of satellite-derived lava discharge rates at Etna: Implications for steady volumetric output, *J. Geophys. Res.*, *116*, B08204, doi:10.1029/2011JB008237.

1. Introduction

[2] Many persistently active basaltic volcanoes undergo variations in effusive output spanning time scales of days to months [e.g., *Frazzetta and Romano*, 1984; *Harris et al.*, 1997; *Harris and Neri*, 2002; *Lautze et al.*, 2004]. These variations may reflect magma supply conditions, such as the waxing-and-waning trend observed when a pressurized volume is tapped [e.g., *Wadge*, 1981; *Harris et al.*, 2000; *Rowland et al.*, 2003], or pulsed supply causing surges in effusion [e.g., *Bailey et al.*, 2006; *James et al.*, 2010; *Favalli et al.*, 2010]. However, at persistently active systems, such relatively short-term variations are often lost in longer-term records that instead show remarkably stable output rates over decadal scales, consistent with steady state behavior [e.g., *Wadge et al.*, 1975; *Allard et al.*, 1994; *Wadge et al.*, 2010].

[3] For Mt. Etna (Sicily, Italy), *Wadge and Guest* [1981] showed that, between 1971 and 1981, although being erupted as part of 37 discrete effusive eruptions, output was marked by a linear decadal-scale trend, with lava being erupted at an average rate of 0.7 m^3 s^{-1}. This trend also characterized the 1980s and 1990s, an average output rate of around 1 m^3 s^{-1} being apparent in the erupted volume data for 1975–1995 given by *Allard* [1997]. However, a change in eruption style was witnessed during the flank eruption of July-August 2001. This event was marked by an anomalous degree of explosivity, as well as by an eccentric eruption of a fast rising, volatile-rich batch of amphibole-bearing magma which contrasted with activity styles witnessed during the preceding 30 years [*Calvari and the Whole Scientific Staff of INGV-Sezione di Catania*, 2001; *Behncke and Neri*, 2003a; *Corsaro et al.*, 2007]. This 2001 eruption was followed by a further eccentric eruption in 2002, during which explosivity was again remarkably high [*Spampinato et al.*, 2008]. This has led some to suggest that the supply and eruption dynamics at Etna were changing, with the 2001 event initiating this change [*Allard et al.*, 2006; *Behncke and Neri*, 2003a; *Clocchiatti et al.*, 2004].

[4] Such a hypothesis can be tested using long-term discharge rate records. For Etna, such a record exists, and is represented by the archive of thermal data available from the satellite-borne sensor, the Advanced Very High Resolution Radiometer (AVHRR). This data set now spans 30 years, and dates back to the launch of the first AVHRR sensor on 13 October 1978 [*Cracknell*, 1997]. These data allow extraction of time-averaged lava discharge rates following the methodology of *Harris et al.* [1997]. Such measurements can be made at a minimum temporal resolution of 12 h, the return period of the NOAA satellites on which AVHRR is flown. For the period 1980 to 2010, we have identified

[1]Laboratoire Magmas et Volcans, Université Blaise Pascal, Clermont-Ferrand, France.
[2]HIGP, SOEST, University of Hawai'i at Mānoa, Honolulu, Hawaii, USA.
[3]Istituto Nazionale di Geofisica e Vulcanologia, Catania, Italy.

0148-0227/11/2011JB008237

Table 1. New, Old, and Modified Old Relations Used to Convert Active Lava Area to TADR at Etna Using AVHRR and MODIS Data[a]

Relation	Temperature Condition (°C)
Old	
$TADR_{min}$ (m^3 s^{-1}) = 2.5×10^{-6} (m s^{-1}) A_{max} (m^2)	100
$TADR_{max}$ (m^3 s^{-1}) = 43×10^{-6} (m s^{-1}) A_{min} (m^2)	500
New	
$TADR_{min}$ (m^3 s^{-1}) = 5.5×10^{-6} (m s^{-1}) A_{max} (m^2)	100
$TADR_{max}$ (m^3 s^{-1}) = 150×10^{-6} (m s^{-1}) A_{min} (m^2)	600
Modified old	
$TADR_{min}$ (m^3 s^{-1}) = 1.7×10^{-6} (m s^{-1}) A_{max} (m^2)	100
$TADR_{max}$ (m^3 s^{-1}) = 162×10^{-6} (m s^{-1}) A_{min} (m^2)	1000

[a]The second column gives the temperature condition used to apply the mixture model of equation (2) and hence to supply the required area value for each relation.

1792 cloud-free images spanning 23 eruptions at Etna, yielding a data set capable of testing the hypothesis and detailing any variation in the rate of output over time.

2. Method and Data

2.1. Method

[5] *Harris et al.* [1997] presented a method for obtaining time-averaged lava discharge rate (TADR) from satellite thermal infrared data. This was initially tested using AVHRR data collected during Etna's 1991–1993 eruption. The method reduces to the application of an empirical relation that allows TADR to be obtained from a measure of active lava area [*Wright et al.*, 2001]. The derived discharge rate then relates to the time-averaged flux required to spread the lava over a given area. The method uses one band of data collected in the thermal infrared, typically between 10 μm and 12 μm, and applies a simple mixture model to the pixel-integrated spectral radiance to extract lava area (R_{TIR}). To do this, the pixel is assumed to contain a mixture of lava-free land and active lava so that, if the temperatures of the two components are assumed, the pixel portion occupied by the two components can be calculated using the pixel-integrated radiance, which is written:

$$R_{TIR} = p_{lava}R_{lava} + p_{land}R_{land} \quad (1)$$

where R_{lava} and R_{land} are the spectral radiances for the lava and lava-free land surfaces, and p_{lava} and p_{land} are the pixel portions occupied by these two components. Note that p_{lava} and p_{land} must sum to one, so that p_{land} can also be written $1 - p_{lava}$. Now, if we can assume values for R_{lava} and R_{land}, we can calculate the pixel portion occupied by active lava from:

$$p_{lava} = (R_{TIR} - R_{land})/(R_{lava} - R_{land}). \quad (2)$$

[6] Following *Harris et al.* [1997], the radiance of the lava-free land can be obtained from surrounding, active lava-free pixels, and the lava surface radiance can be assumed over a range of radiances (obtained from the equivalent temperature range). The result yields a range of pixel portions occupied by the lava, ranging from a maximum value obtained with the maximum assumed lava temperature, to a minimum value obtained with the minimum assumed lava temperature. Multiplying the pixel portions by pixel area, and summing for all hot pixels containing active lava, gives the active lava area.

[7] Now, the active area can be used to estimate the TADR required to feed flow over the given area (A) using an empirical relation initially proposed by *Pieri and Baloga* [1986]. The relation reduces to a linear trend whereby [*Wright et al.*, 2001; *Harris and Baloga*, 2009]:

$$TADR = xA \quad (3)$$

in which x is the coefficient that defines a positive, linear relation between TADR and A. Two relations are required, one for the maximum estimated flow area (A_{max}) and one for the minimum estimated flow area (A_{min}). This yields a range of TADRs, between which the actual value usually lies. The relation is best set through best fitting through calibration using ground-measured values [*Harris et al.*, 2010]. For effusive eruptions at Etna between 1980 and 1999, the relation labeled "*old*" in Table 1 provided good fits with field measured values when used with A_{max} obtained assuming a typical lava surface temperature of 100°C and A_{min} assuming 500°C [*Harris et al.*, 1997, 2000, 2007]. However, best fitting using TADRs derived from LIDAR data collected simultaneously with satellite passes during Etna's 2006 eruption yielded a different best fit relation for this eruption; this relation is labeled "*new*" in Table 1. For this new case A_{max} obtained assuming a typical lava surface temperature of 100°C and A_{min} assuming 600°C provided the best fit with the LIDAR data [*Harris et al.*, 2010]. For each eruption we thus apply a range of conversion cases, and use the case which provides the best fit between satellite-data-derived and field-measured TADR. Based on best fitting using ground-based data acquired during Etna's 1999 eruptions at the SE Crater and Bocca Nuova, we also applied a modified version of the old relation, as given in Table 1. This "*modified old*" relation uses with A_{max} obtained assuming a typical lava surface temperature of 100°C and A_{min} assuming 1000°C [*Harris and Neri*, 2002].

[8] We apply these conversions to (1) generate TADR time series for each eruption for which satellite data are available during the period 1980–2010 and (2) assess, through comparison with independent field measurements of TADR, which best fit relation applies to each eruption (as done in Figures 1–3). We use these data to volumetrically characterize each eruption in terms of the TADR trend, as well as the maximum and mean TADRs that feed each eruption. By integrating the TADRs for each eruption (using

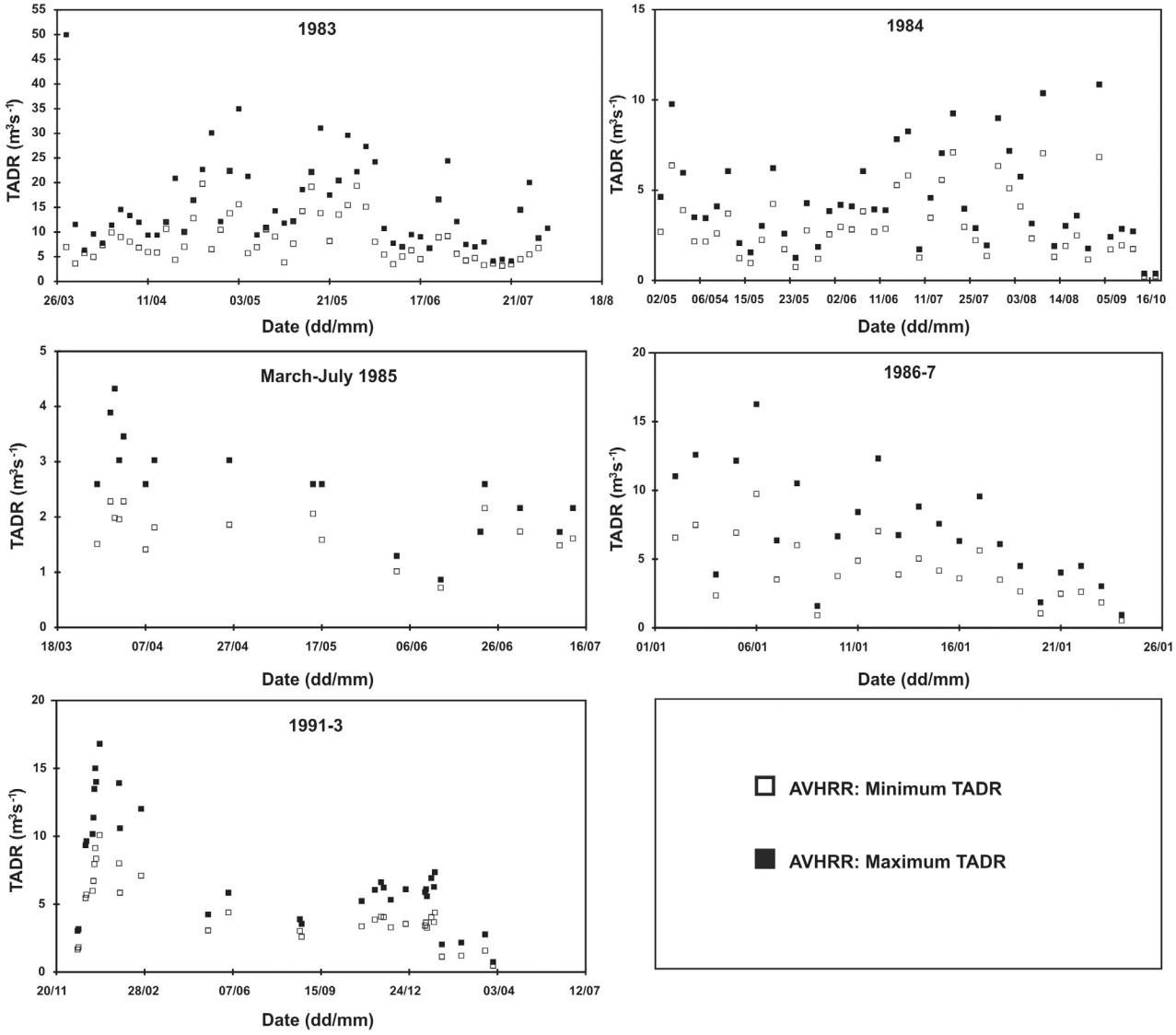

Figure 1. Satellite-data-derived TADR time series for each major (>10^7 m^3) effusive eruption at Etna during the period 1980 to 1993.

trapezium rule) we also provide an estimate for the volume erupted during each eruption, as well as the mean output rate (MOR) for each eruption, this being the total volume erupted divided by the eruption duration [*Harris et al.*, 2007]. We can thus use our data set to define each effusive eruption in terms of intensity (maximum TADR) and magnitude (total volume erupted).

2.2. Data

[9] To apply the methodology described above we used all AVHRR data obtained by the University of Dundee (Dundee, Scotland) receiving station between 1980 and 2010. Following *Harris et al.* [1997], we used the band 4 (10.3–11.3 μm) pixel-integrated temperatures, where all data were calibrated and corrected for nonlinearity effects [e.g., *Brown et al.*, 1993; *Weinreb et al.*, 1990; *Kidwell*, 1995] by the NERC based at the Plymouth Marine Laboratory (Plymouth, UK). Data were then corrected for atmospheric and emissivity effects, and pixel areas were calculated as a function of the sensor instantaneous field of view and scan angle. Data between 10 and 12 microns need to be corrected for atmospheric upwelling radiance (R_{up}), atmospheric transmissivity (τ) and surface emissivity following (ε):

$$R_{TIR} = \left(R_{sat} - R_{up}\right)/\tau\varepsilon \quad (4)$$

R_{sat} being the at-satellite radiance. We estimated R_{up} and τ as a function of scan angle using the MODTRAN atmospheric code, where typical values for a surface at an altitude of 0 m (at nadir and using a U.S. Standard atmosphere), averaged between 10 and 12 μm, are 1.79×10^{-5} W cm^{-2} sr^{-1} μm^{-1} and 0.96, respectively. Emissivity averaged over the same wave band is also 0.96 (obtained from reflectance spectra for a sample of Etna 'a'a).

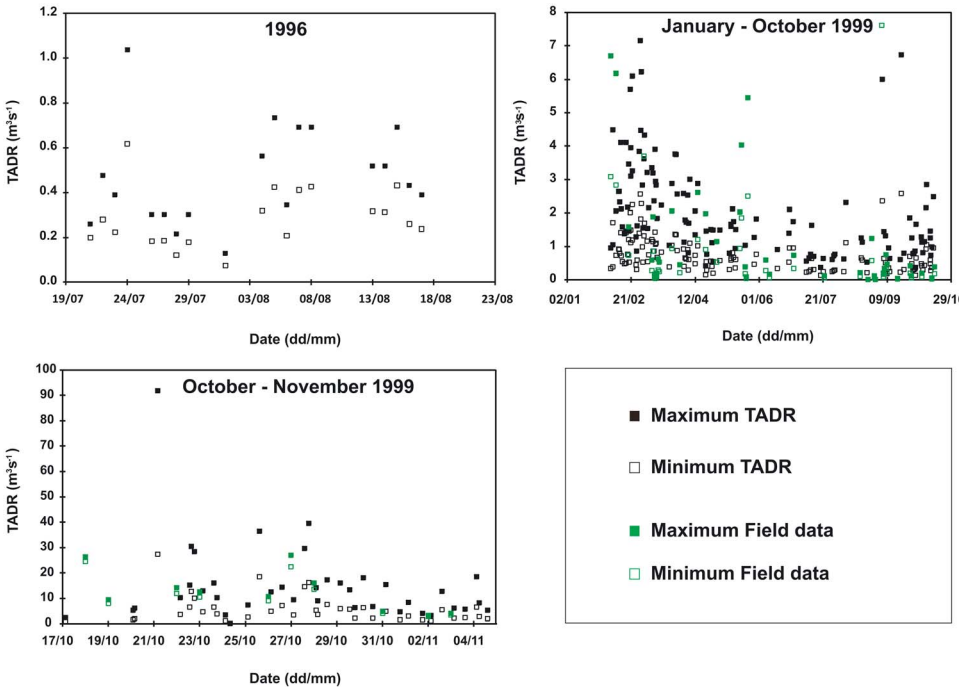

Figure 2. Satellite-data-derived TADR time series for each major (>10^7 m^3) effusive eruption at Etna during the period 1996 to 1999.

[10] For the period 2000–2010, we also used data from band 31 (10.78–11.28 μm) of the Moderate Resolution Imaging Spectroradiometer (MODIS) [*Salomonson et al.*, 1989; *Barnes et al.*, 1998]. This sensor was first launched in 1999, and provides data with a similar spatial and temporal resolution to the AVHRR, and at a similar wavelength. These data were processed in the same way. Here, the full database is, for the first time, collated in one place (see auxiliary material).[1] While the pre-1993 portion of this database was processed by *Harris* [1996], all post-1999 data were processed by Hawaii Institute of Geophysics and Planetology staff during various eruption crises and transmitted to Istituto Nazionale di Geosfisica e Vulcanologia-Sezione di Catania, as well as Centro Nazionale Terremoti (Rome), during those crises [*Harris et al.*, 2007]. All data have been reprocessed here to check for correct application of TADR conversion coefficients (see auxiliary material).

[11] The main effusive events that occurred at Etna between 1980 and 2010 are listed in Table 2, along with their location, duration and number of available AVHRR and MODIS images. We see that there were around 36 effusive events, of which 25 lasted more than 1 day. During the period, AVHRR and MODIS data were available for 23 events, the remaining events being too short to capture, given the 12 h separation of AVHRR and MODIS passes, or because of cloud cover. For these 23 events, 1792 images were available of which 509 were from MODIS. We see that a total of 16 events comprise data sets of more than 10 images, allowing TADR time series to be generated for all of the main effusive events, with the exception of those occurring during 1997–1998, for which we have no satellite data (see Table 2). We also collated all available lava flow volume data for the period 1971–2010, as given in Appendix A. This allowed us to fill all of the gaps in the satellite-derived record.

3. Results

[12] The satellite-derived TADR time series for each effusive eruption are given in Figures 1–3. The full database on which these plots and following treatments are based are given, for each major effusive eruption listed in Table 3, as data files in the auxiliary material.

3.1. Classification of Eruptions on the Basis of Satellite-Derived TADR Trends

[13] Using our satellite-derived TADR time series we define four types of effusive event on the basis of characteristic trends in the TADR time evolution during each eruption. Type I and II trends were defined by *Harris et al.* [2000] using the 1980–1996 portion of this data set and involve the following trends:

[14] 1. Type I trends are characterized by a rapid waxing phase, followed by a longer waning phase, and are consistent with tapping of a pressurized volume [*Wadge*, 1981]. In Type I eruptions ~50% of the volume is typically erupted in the first ~25% of the total eruption time. Five eruptions show Type I trends, these being the eruptions of 1983, 1986–1987, 1991–1993, 2002–2003 and 2008–2009 (Figure 4a).

[15] 2. Type II trends are characterized by relatively stable and low TADRs that span 0.1 and 5 m^3 s^{-1}, with ~50% of the volume erupted in ~50% of the total eruption time. Type II trends tend to be associated with summit eruptions. They are thus consistent with nonpressurized overflow from the summit craters. Four eruptions show Type II trends,

[1] Auxiliary materials are available at ftp://ftp.agu.org/apend/jb/2011jb008237.

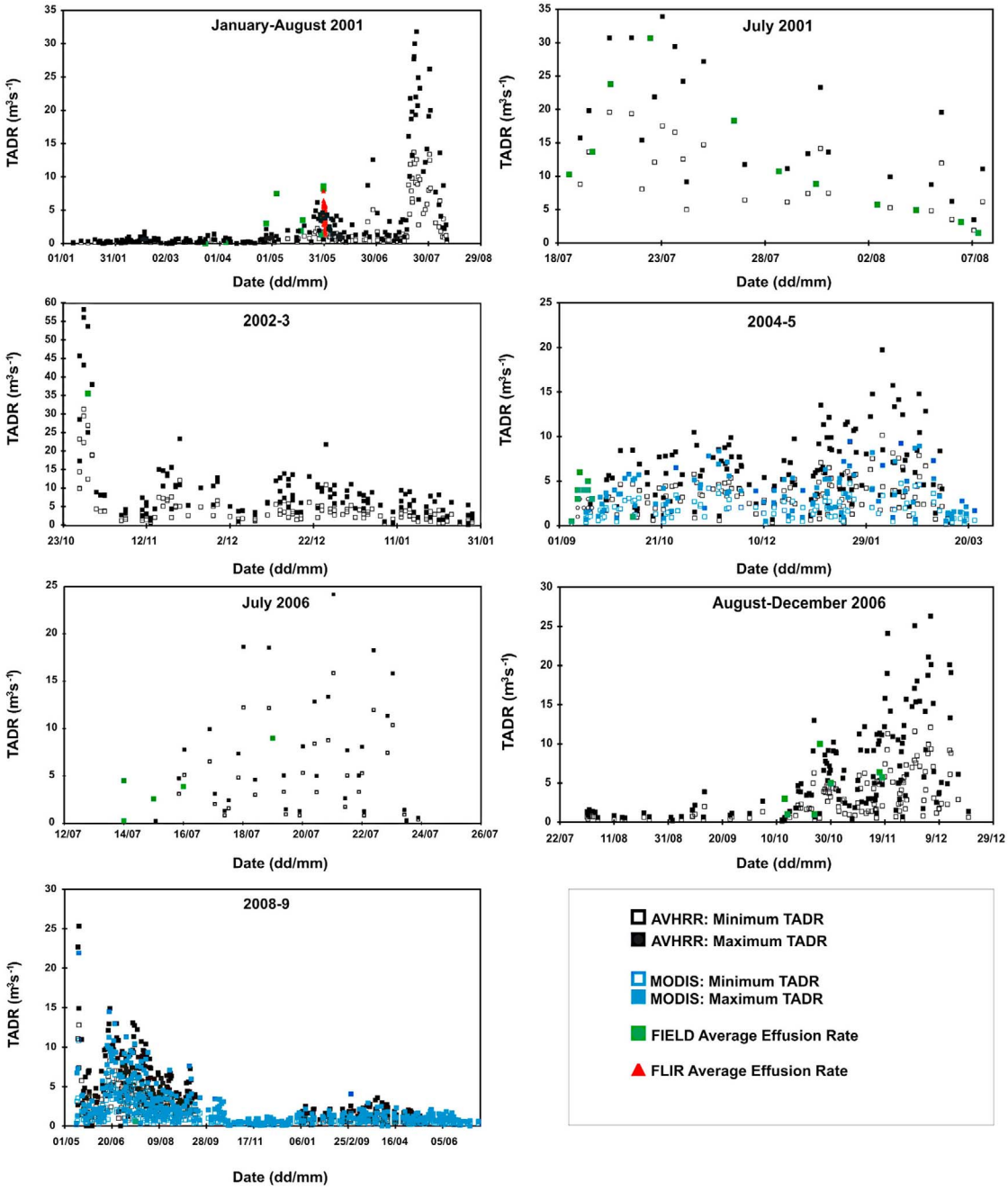

Figure 3. Satellite-data-derived TADR time series for each major (>10^7 m^3) effusive eruption at Etna during the period 2000 to 2010.

these being the eruptions of 1984, 1985, 1996 and 1999's SE Crater eruption (Figure 4b).

[16] In new data processed for the post-2000 period we find two other trends, Types III and IV. Of these two trend types, the Type III trend has been described, and explained, by *Steffke et al.* [2011] through comparison of satellite-derived TADRs and ground-measured SO_2 fluxes for the 2004–2005 and 2006 eruptions; the Type IV trend has been examined by *Harris and Neri* [2002], whereby:

[17] 3. Type III trends are characterized by TADRs that increase with time and are associated with three eruptions, those of the SE Crater in 2001, plus those of 2004–2005 and August-December 2006 (Figure 4c). This trend likely results from the ascent of a magma batch which pushes a volume of degassed magma ahead of it, and is consistent with an imbalance observed between TADRs and SO_2 emission rates during the opening phase of the 2004–2005 eruption [*Steffke et al.*, 2011]. Eruption of the degassed volume contributes to the opening, low TADR, phase; arrival of the ascending batch contributes to the high TADR terminating phase.

[18] 4. Type IV trends are extremely pulse-like. Peaks in such trends are of high amplitude and attain values of 10s to

Table 2. Main Effusive Eruptions at Etna, 1980–2010[a]

Eruption	Location	Start Date (dd-mm-yy)	Stop Date (dd-mm-yy)	Duration (days)	Ground-Based Measurements (Source[b])	Number of AVHRR and MODIS Images
1980 (1 Sep)	NE crater	01-09-80	01-09-80	<1		0
1980 (6 Sep)	NE crater	06-09-80	06-09-80	<1	1	0
1980 (26 Sep)	NE crater	26-09-80	26-09-80	<1		0
1981 (Feb)	NE crater	05-02-81	07-02-80	2		1
1981 (Mar)	NW flank	17-03-81	23-03-81	5		3
1983	S flank	28-03-83	06-08-83	131	2	54
1984	SE crater	27-04-84	16-10-84	172		45
1985 (Mar)	SE crater	08-03-85	11-03-85	1		0
1985 (Mar-Jul)	S flank	12-03-85	13-07-85	124	1	17
1985 (Dec)	E flank	25-12-85	31-12-85	6		1
1986	NE crater	14-10-86	24-10-86	14		0
1986–1987	E flank	30-10-86	27-02-87	120		23
1989 Sep	SE crater	11-09-89	27-09-89	17		5
1989	E flank	27-09-89	09-10-89	11		3
1990 (4–5 Jan)	SE crater	04-01-90	05-01-90	<1		0
1990 (12 Jan)	SE crater	12-01-90	12-01-90	<1		0
1990 (14–15 Jan)	SE crater	14-01-90	15-01-90	<1		0
1990 (1–2 Feb)	SE crater	01-02-90	02-02-90	<1		0
1991–1993	E flank	14-12-91	30-03-91	471	3	33
1996	NE crater	21-07-96	19-08-96	29	7	19
1997–1998	SE crater	03-97	07-97	518		N/A
1998	SE crater	22-07-98	22-07-98	<1		N/A
1998–1999	SE crater	15-10-98	23-01-99	131		N/A
1999	SE crater	04-02-99	14-11-99	283	4	123
1999	Bocca Nuova	17-10-99	05-11-99	19	5	39
2000	SE crater	26-01-00	24-06-00	151		
2001	SE crater	21-01-01	17-07-01	177	6	207
2001	S flank	17-07-01	09-08-01	23	7	33
2002	NE flank	27-10-02	05-11-02	9	10	14
2002–2003	S flank	27-10-02	29-01-03	94	10	122
2004–2005	SE crater	07-09-04	08-03-05	182	8 and 10	233
2006 (Jul)	SE crater	14-07-06	24-07-06	10	10	30
2006	SE crater	12-10-06	14-12-06	63	9 and 10	129
2007 (29 Mar)	SE crater	29-03-07	29-03-07	<1		1
2007 (11 Apr)	SE crater	11-04-07	11-04-07	<1		1
2007 (29 Apr)	SE crater	29-04-07	29-04-07	<1		0
2007 (6 May)	SE crater	06-05-07	06-05-07	<1		0
2007 (4–5 Sep)	SE crater	04-09-07	05-09-07	2		0
2008–2009	SE crater	13-05-08	07-07-09	420	10	656

[a]Pre-1999 details are from *Harris et al.* [2000, Tables 1 and 3].

[b]Sources are numbered as follows: 1, *SEAN* [1989]; 2, *Frazzetta and Romano* [1984]; 3, *Calvari et al.* [1994]; 4, *Calvari et al.* [2003]; 5, *Harris and Neri* [2002]; 6, *Lautze et al.* [2004]; 7, *Coltelli et al.* [2007]; 8, *Neri and Acocella* [2006]; 9, *Harris et al.* [2010] and *Favalli et al.* [2010]; 10, INGV internal reports.

Table 3. Volumetric Characteristics for the Main (Greater Than 2 Days Long) Effusive Events Spanning 1983 Through 2010[a]

Period	Eruption	E_r-A Relation	Maximum TADR ($m^3\ s^{-1}$)	Typical TADR ($m^3\ s^{-1}$)	TADR Temporal Trend (Type)
1	1983	old	35	11.5	I
1	1984	old	11	3.7	II
1	1985 (Mar-Jul)	old	4	2.1	II
1	1986–1987	old	16	5.7	I
1	1991–1993	old	17	5.9	I
2	1996	old	1	0.4	II
2	1999 (SEC)	modified old	7	1.4	II
2	1999 (BN)	modified old	92	10.2	IV
3	2001 (SEC)	new	32	3.1	III
3	2001 (S. flank)	new	56	22.1	IV
3	2002	new	58	23.7	I
3	2002–2003	new	23	5.3	I
3	2004–2005	new	20	4.0	III
3	2006 (Jul)	new	24	6.1	IV
3	2006	new	26	5.1	III
3	2008–2009	new	25	2.5	I

[a]See auxiliary material for further details of each event.

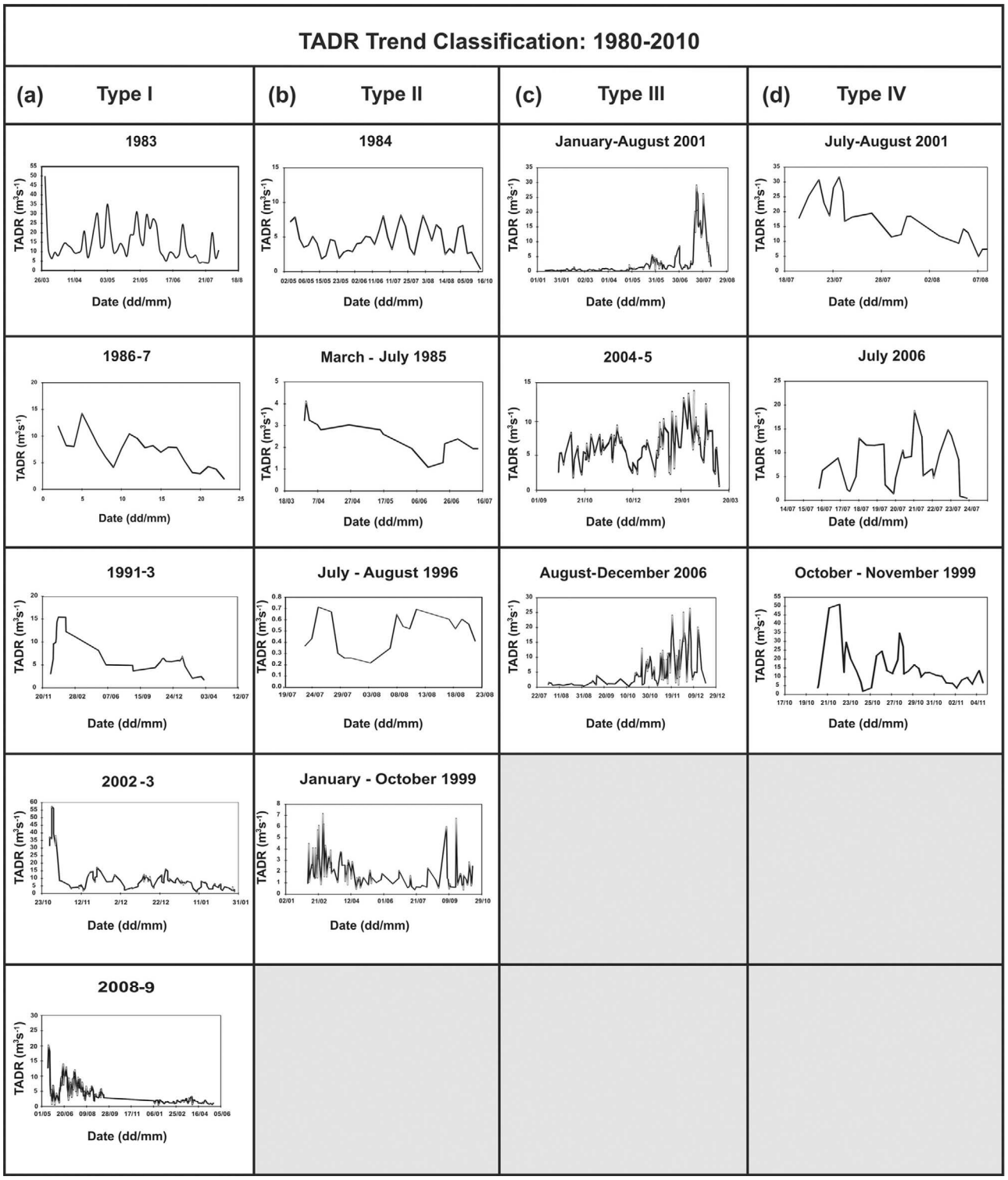

Figure 4. Classification of TADR time series given in Figures 1–3 by trend type. TADRs smoothed with a two-point running mean calculated for the maximum TADR bound are given so as to highlight the dominant trend.

100s of meters cubed per second. Such trends likely relate to the rise and eruption of a series of rapidly ascending magma batches. The first eruption of this type was the October-November 1999 eruption of the Bocca Nuova. This event was marked by 11 discrete paroxysmal events during which intense strombolian and lava fountain activity fed vigorous channelized 'a'a lava flows at TADRs of up to 120 m^3 s^{-1} [*Harris and Neri*, 2002]. Two other eruptions show this Type IV trend, those being the July-August south flank eruption of 2001, plus the July 2006 eruption (Figure 4d).

Table 4. Volumetric Characteristics for the Two Main Periods of Effusive Events Identified Between 1980 and 2010[a]

Period	Eruption	Duration (days)	Volume ($\times 10^6$ m)	Mean Output Rate ($m^3\ s^{-1}$)
1	1983	131	103	9.1
1	1984	172	46	3.1
1	1985 (Mar-Jul)	124	18	1.7
1	1986–1987	120	49	4.7
1	1991–1993	471	183	4.5
Total (number = 5)		1018	399	4.5
Mean		204	80	4.6
3	2001	177	17	1.1
3	2001	23	38	19.2
3	2002–2003	94	50	6.2
3	2004–2005	182	64	4.1
3	2006 (Jul)	10	2	2.0
3	2006	63	37	6.9
3	2008–2009	420	68	1.9
Total (number = 7)		969	276	3.3
Mean		138	39	5.9
3b	2001	23	38	19.2
3b	2002–2003	94	50	6.2
3b	2004–2005	182	64	4.1
3b	2006 (July)	10	2	2.0
3b	2006	63	37	6.9
Total (number = 5)		372	191	5.9
Mean		74	38	7.6

[a]Period 3b is the same as period 3 but without the two long-duration SE Crater eruptions that began and ended the period. Volumes are obtained from integrating the midpoint TADR value though time. For each period, mean output rate has been calculated by dividing the total volume emplaced by all eruptions during each period by the total duration of all activity during the same period. This is given on the "total" line below each period. Also given is the mean MOR for individual eruptions within each period (given on the "mean" line below each period).

3.2. Time Distribution of Effusive Event Types

[19] If we examine the distribution of events by Type through time we find that all of the large ($>10^7$ m^3) volume eruptions prior to 1999 involved eruptions with Type I or II trends (Table 3), as already described by *Harris et al.* [2000]. Note, though, that we reclassify Etna's February-November 1999 eruption. This eruption was originally classified as Type I by *Harris et al.* [2000]. This assignment was made on the basis of a limited data set. However, processing of the full AVHRR data set available for this eruption reveal a Type II, slowly oscillating, trend as also found in the field-derived TADRs of *Calvari et al.* [2003]. In contrast, the Bocca Nuova eruption that occurred in the same year, during October and November, had a strongly pulsating character, as detailed by *Harris and Neri* [2002], meaning that we here classify this eruption as Type IV. We also note that the opening, high TADR, phase of the 1983 eruption was missing from the AVHRR-derived data set due to cloud cover. The opening phase was, however, recorded by *Frazzetta and Romano* [1984] whose field data clearly show this eruption to be of Type I character. Thus, *Frazzetta and Romano*'s [1984] field-derived TADR for this opening phase have been added to the plot in Figure 4 to justify its classification as Type I.

[20] Type III and IV trends dominate from 1999 onward (Table 3). The first event in this series, the January-July 2001 eruption of the SE Crater, shows a series of oscillations which, as detailed by *Lautze et al.* [2004], increase in amplitude toward the July-August 2001 flank eruption. These oscillations lend a Type III character to the January-July 2001 eruption. Such Type III behavior is then also apparent during the July 2006 eruption of the SE Crater. Of the remaining post-2001 eruptions, both the eruptions of 2004–2005 and August-December 2006 show TADRs that build toward the end of the eruption, giving them also a Type III trend. The remaining two eruptions of this period are the 2002–2003 and 2008–2009 eruptions, which both have Type I trends.

[21] It is worth stressing that, although Type II and IV trends may look similar, the two classes are distinguished by the range of variability during pulses that interrupt the otherwise flat trends. For Type II trends the pulses generally have ranges of between ~1 and 7 $m^3\ s^{-1}$, whereas pulses in Type IV trends have ranges of up to 100 $m^3\ s^{-1}$. As noted above, the TADR levels are also quite different between Type II and IV events.

[22] Finally, we have classified the eruptions based on the dominant or primary trend. Several eruptions have secondary trends overprinted on the primary trends. For example, while all Type III trends appear to have Type IV trends overprinted, the Type IV trends of the October-November 1999 and July-August 2001 eruptions also show a secondary declining trend with time, suggestive of a Type I influence. Note too, that the 2002–2003 eruption has been classified as Type I. This is mainly due to the contribution of high TADR flows during the opening phase on the northeast flank. Once these flows shut down, Type II trends are apparent for the following south flank emission.

3.3. Groupings

[23] Calibration factors that need to be used to provide the best fit to independent ground-based TADR estimates, as given in Table 1, produce a grouped data set, with each grouping requiring a different calibration factor to achieve best fit. Each grouping also has distinct and characteristic maximum recorded TADR (Table 3), as well as eruption frequencies, durations, volumes and MORs (Table 4). This

allows us to divide our data into two 11 year long periods on the basis of the volumetric character of the eruptions occurring within each period. These two periods are separated by a third period of low volumetric output, with the two high-volume periods spanning 1983–1993 (Period 1) and 2000–2010 (Period 3).

3.3.1. Period 1: 1983–1993

[24] The first period was marked by four eruptions each involving the output of 10^7 m^3 of lava or more. Durations ranged between 120 and 471 days (mean = 204 days) to emplace lava volumes of between 18 and 183 × 10^6 m^3 (mean = 80 × 10^6 m^3) at mean output rates of 1.7 to 9.1 m^3 s^{-1}, with a mean of 4.6 m^3 s^{-1} (Period 1, Table 4). Maximum TADRs were between 4 and 35 m^3 s^{-1}, with an average of between 2 and 12 m^3 s^{-1} (Table 4).

[25] Best fits with field data, revealed that the "old relation" applied to this series of eruptions, as already detailed by *Harris et al.* [2000]. For example, applying the "old relation" to the 1991–1993 data set and integrating the TADRs through time yields an erupted volume of 183 ± 72 × 10^6 m^3, compared with a volume measured using Electronic Distance Measurement by *Stevens et al.* [1997] of 185 ± 22 × 10^6 m^3.

3.3.2. Period 2: 1994–1999

[26] Following the eruption of 1991–1993, the most voluminous effusive event of the last 3 centuries [*Calvari et al.*, 1994], there was a three year hiatus in effusive activity until 1996 (Appendix A). This period was followed by dominantly intracrater summit activity [*Neri et al.*, 2005; *Allard et al.*, 2006], and then by the two phases of the 1999 eruption (from SE Crater and Bocca Nuova [*Calvari et al.*, 2003; *Harris and Neri*, 2002]). This period involved eight effusive events and was volumetrically transitional between Periods 1 and 3, with the 1999 SE Crater and Bocca Nuova eruptions requiring application of the "modified old relation." The Bocca Nuova eruption also had a particularly high maximum TADR and was the first non-Type I or II event of our series (Table 3). During this 6.75 year long period, 36 × 10^6 m^3 of lava were erupted at a TADR of 0.2 m^3 s^{-1}. *Rothery et al.* [2001] showed an increasing volcanic radiance trend between 1996 and the end of 1999. This would convert to an increasing TADR trend, which builds to culminate in the high-intensity events experienced by the Bocca Nuova in 1999.

3.3.3. Period 3: 2000–2010

[27] The third period was marked by seven eruptions involving the output of 10^7 m^3 of lava or more, with a total erupted volume similar to that of Period 1. However, although the frequency of eruption was higher in Period 3, eruption durations tended to be shorter, with a mean duration of 138 days, compared with a mean of 204 days for Period 1 (Table 4). Volumetrically, the character of the Period 3 eruptions also contrasts with those of Period 1 in that (1) emplaced lava volumes during individual eruptions were smaller, being between 2 and 68 × 10^6 m^3 (mean = 39 × 10^6 m^3) during Period 3, compared with a range of 18 to 183 × 10^6 m^3 (mean = 80 × 10^6 m^3) during Period 1 (Table 4); (2) the shorter durations for Period 3 eruptions meant that MORs were typically higher than during Period 1 eruptions, Period 3 MORs having a mean of 5.9 m^3 s^{-1} compared with 4.6 m^3 s^{-1} during Period 1 (Table 4); and (3) maximum TADRs were higher in Period 3 than during Period 1, being between 20 and 58 m^3 s^{-1}, with an average of between 3 and 24 m^3 s^{-1} during Period 3, compared with a range of 4 and 35 m^3 s^{-1} and averages of between 2 and 11.5 m^3 s^{-1} during Period 1 (Table 3).

[28] These differences are accentuated if we remove the two long-duration SE Crater eruptions that began and ended the period, as done in Table 4 (Period 2b).

[29] Best fits with field data, from the sources indicated in Table 2 and given in the auxiliary material, also revealed that the "old relation" no longer applied to the second period eruptions, with the "new relation" instead applying to all eruptions in this series. For example, applying the "old relation" to the first three months of the 2004–2005 data set and integrating the TADRs through time yields an erupted volume of ~15 × 10^6 m^3, compared with a ground-measured volume of between 18.5 and 32 × 10^6 m^3 [*Burton et al.*, 2005]. However, use of the "new relation" yields a value ~28 × 10^6 m^3, a value more-or-less central to the field-measured volume. Likewise, applying the "old relation" to the TADRs for the lava flow field of the Lower Fissure System at 2100 m a.s.l. (the LFS1 flow field of *Coltelli et al.* [2007]) active during the 2001 south flank eruption, and integrating the TADRs through time, yields an erupted volume of 13 ± 8 × 10^6 m^3. This is low when compared with the volume of 21.4 × 10^6 m^3 acquired from subtraction of digital elevation models generated during the eruption by *Coltelli et al.* [2007]. Instead, use of the "new relation" yields a value of 22.2 ± 6.1 × 10^6 m^3, again in excellent agreement with the target value.

4. Discussion

[30] Good fits between ground-measured volumes and volumes obtained from integrating up to 656 satellite-derived TADRs collected over eruptions lasting up to 500 days indicate that the satellite-based conversion is valid and can be trusted. In the case of the 2008–2009 eruption, for example, any systematic error in our TADRs would yield a large error in the final volume estimate obtained from integrating 656 TADRs over 420 days. However, the satellite-data-derived volume of 68 × 10^6 m^3 is identical to the ground measured volume, and backs up our good fits between the ground-measured and satellite-TADR-derived volumes for the 1991–1993, 2001 and 2002–2005 lava flow fields. These data have now been collected over 30 years and used to track and assess effusion rates during individual eruptions [*Harris et al.*, 1997; *Harris and Neri*, 2002; *Lautze et al.*, 2004; *Harris et al.*, 2007; *Vicari et al.*, 2009; *Harris et al.*, 2010]. Here, these data are collated allowing them to be used as a resource to statistically define and track Etna's longer-term volumetric output behavior.

[31] Our analysis of this database shows a change in the eruptive style, defined by volumetric properties, following the 2001 eruption (as seen in Tables 3 and 4). We find that, while the period 1983–1993 was characterized by less frequent, but longer-duration effusive eruptions at lower TADRs, 2000–2010 was characterized by more frequent effusive eruptions of shorter duration and higher TADRs. Another important difference is the mean lava volume of eruptions, the mean volume for eruptions between 1983 and 1993 being a factor of two higher than those for eruptions between 2000 and 2010, being 80 × 10^6 m^3 for the former

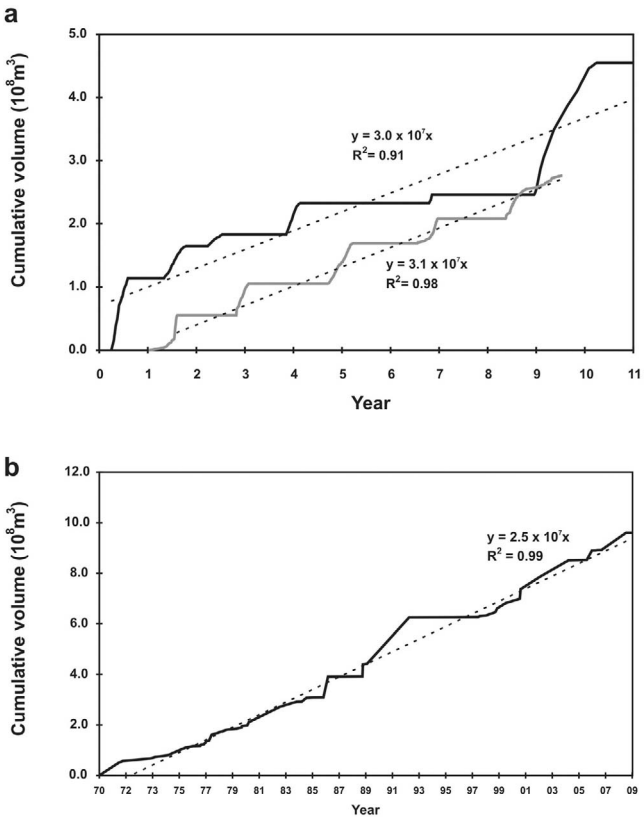

Figure 5. (a) Cumulative volume plots for 1983–1993 (black) and 2000–2010 (gray). Each is plotted as a function of years since the beginning of each 11 year long period. (b) Cumulative volume plot for the period 1970–2010 generated using the volume data given in Appendix A. For each plot, the $y = m\,x$ linear best fit is given, where the m value is given in units of cubic meters per year.

period and 39×10^6 m^3 for the latter (Table 4). This change begins with the activity of 2001, suggesting that this year marked a change in the volumetric style of effusion. This change in activity style has already been explored in several previous studies which point to the increased explosivity and different chemistry of the erupted products during 2001 and 2002–2003 [*Behncke and Neri*, 2003a; *Clocchiatti et al.*, 2004; *Métrich et al.*, 2004; *Corsaro et al.*, 2007]. After 2001, a new relation also has to be applied to our satellite data to derive TADRs that fit well with ground-based data. This new relation, as well as the old relation, is given in Table 1. If we compare the two relations we see that, to obtain the same areal coverage as was achieved using the old relation, a higher TADR is required in the new relation. This suggests a rheological change in the erupted lava, where an increase in viscosity and/or yield strength would force a decrease in the area over which a given volume of lava could spread at any given TADR. That all eruptions from 2001 onward required this new relation indicates that all lavas erupted since 2001 were subject to these new conditions. In addition, the time variation in TADR witnessed during each eruption changed from 2001 onward, with their Type III and IV trends being more consistent with batch-like ascent, as opposed to the pressurized or overflow-fed release of central conduit magma that generated the Type I and II trends of the first, 1983–1993, period. Together, these changes are consistent with more efficient ascent of batches from depth during 2001–2010, to erupt lava with a modified rheology and output rate when compared with the 1983–1993 period. This change may have been aided by the opening up of surface pathways for magma ascending from the deep source, to result in pathways which bypassed the central conduit and generated eccentric eruptions, as in 2001 and 2002–2003. This has been argued to be facilitated by processes such as flank slip [*Acocella et al.*, 2003; *Neri et al.*, 2005; *Solaro et al.*, 2010; *Ruch et al.*, 2010].

[32] However, in terms of long-term output nothing changed over the 1980–2010 period. If we plot the cumulative lava volumes for the two 11 year long periods spanning 1983–1993 and 2000–2010 we witness identical slopes (Figure 5a), meaning that the time-averaged output over the two periods was the same. As a result, the effused volume built at a steady, time-averaged rate of between 0.7 and 0.9 m^3 s^{-1} which was stable through 2001. Thus, output remained steady even through the major change in style and location of surface emissions that occurred in 2001. Even the movement of Etna's eastern flank [*Ruch et al.*, 2010; *Solaro et al.*, 2010], responsible for the triggering of the 2004–2005 flank eruption [*Burton et al.*, 2005; *Neri and Acocella*, 2006], did not produce any response in the long-term supply, as plotted in Figure 5. All that changed was the way in which this volume was partitioned between, and during, individual effusive events, as well as the spreading properties of the erupted lava.

[33] The steady output rate recorded between 1980 and 2010 has a time-averaged average value of 0.8 m^3 s^{-1}. This is similar to the value of 0.7 m^3 s^{-1} obtained by *Wadge and Guest* [1981] for the period 1973 to 1980. We can thus confirm that this trend has remained constant at least since 1971, as is apparent if we plot our data together with that of *Wadge and Guest* [1981], as done in Figure 5b. Going further back still, we can use the data of *Wadge et al.* [1975] to compare the 1971–2010 trend with those trends in operation since 1550, as done in Figure 6. The period prior to 1971 has already been examined by *Wadge et al.* [1975] who pointed to two main segments in the cumulative volume plot: (1) a segment spanning 1610 to 1669 characterized by a relatively high output rate of 0.8 m^3 s^{-1} and (2) a segment spanning 1759 to 1959 characterized by lower output rates of 0.2 m^3 s^{-1}. We note that the *Wadge et al.* [1975] estimates for 1669–1971 were largely based on flank eruptive volumes. Instead, post-1971 volumes are much closer to a complete flank + summit budget. As discussed by *Wadge and Guest* [1981] the flank-only rate for 1759–1970 was 0.17 m^3 s^{-1}, rising to 0.39 m^3 s^{-1} if the 1971–1981 flank/summit ratio is used. Given this uncertainty, a better value for the second segment would thus be 0.2 ± 0.1 m^3 s^{-1}.

[34] It is noteworthy that, since 1971, we have returned to a trend identical to that witnessed prior to the 1669 eruption. This new trend has now been stable over 40 years. Indeed, if we consider the period 1971–2010 we find that 960×10^6 m^3 of lava was erupted onto the flanks of the volcano in 40 years, with the volume being fairly evenly partitioned between these four decades (Table 5) to define a linear trend in cumulative output, which increases at a time-averaged rate of 0.8 m^3 s^{-1} (Figure 5).

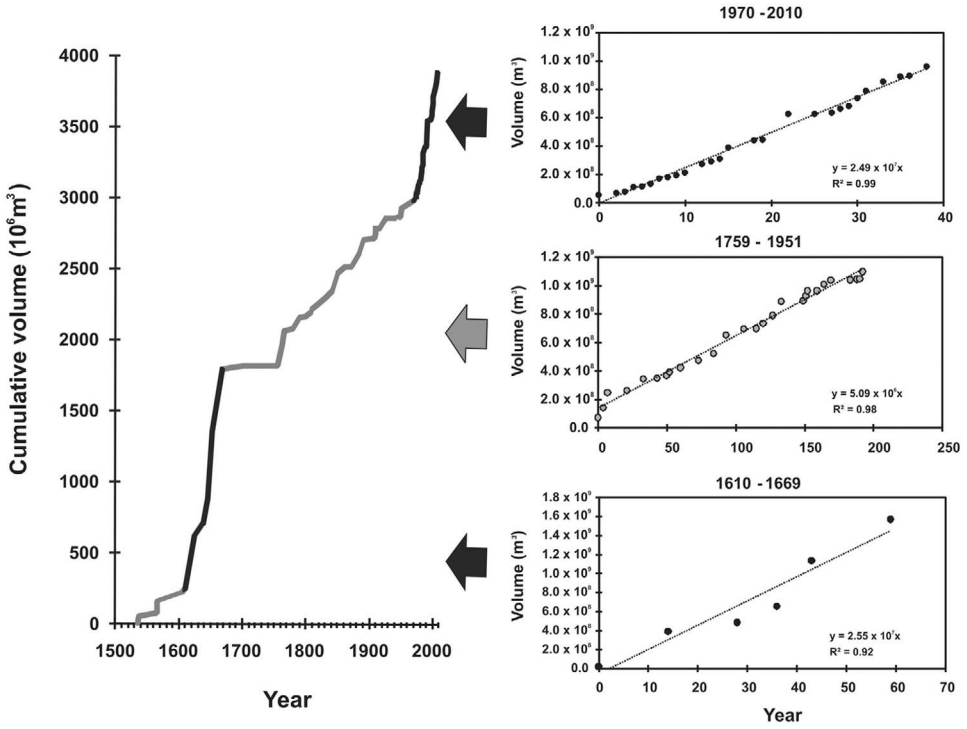

Figure 6. Cumulative volume plot for 1500–2010, with the main output phases distinguished (high-output phases are in black, and low-output phases are in gray). Data for 1610–1970 are from *Wadge et al.* [1975], and those for 1970–2010 are from Appendix A. Cumulative volume as a function of years since the beginning of each phase is given to the left, with the $y = m\,x$ linear best fit for each phase, m being given in units of cubic meters per year.

[35] During the high output rate phase of 1610–1669, eruptions were dominated by flank events [*Wadge et al.*, 1975]. This phase was terminated by the effusive eruption of 1669. The 1669 eruption was the largest historical eruption recorded at Etna in terms of magnitude and intensity, with ~1 km^3 of lava being erupted in about four months of eruption (MOR ≈ 100 $m^3\ s^{-1}$), to build a ~17.5 km long tube-fed lava flow field that reached the sea south of Catania, destroying part of the city [*Corsaro et al.*, 1996; *Crisci et al.*, 2003]. This eruption signaled the end of an eruptive cycle that had lasted a few centuries and that had erupted plagioclase-rich lava, resulting from crystallization of a magma stored at shallow levels within the volcanic pile [*Guest and Duncan*, 1981; *Corsaro et al.*, 1996]. After the 1669 eruption, emptying of the shallow system resulted in a caldera collapse of the summit area [*Guest*, 1973]. The volcanic activity that followed was significantly different in terms of both composition and volumes of lava erupted [*Wadge et al.*, 1975; *Tanguy*, 1980; *Guest and Duncan*, 1981; *Clocchiatti et al.*, 1988; *Hughes et al.*, 1990; *Condomines et al.*, 1995; *Corsaro et al.*, 1996]. At the same time, the style of eruptive activity changed, with the new period showing an increasing number of summit eruptions [*Wadge et al.*, 1975], as well as the lower time-averaged output rates apparent in Figure 6.

[36] The transition back to a high output rate period was heralded by the 1971 eruption [*Wadge and Guest*, 1981], followed a period of reorganization of the summit area, and coincided with the formation of the SE Crater. *Guest* [1973] maps the development of a fissure that cut the summit with a NW-SE trend in 1956. This fissure eventually joined the Bocca Nuova and SE Craters, with the Bocca Nuova opening in 1968 at the NW end of the fissure, and the SE Crater forming at the SE end in 1971. The opening of the SE Crater coincides with the beginning of the modern, high output rate period. As noted by *Branca and Del Carlo* [2004], this period was marked by an increase in summit activity, but also by

Table 5. Erupted Lava Volumes and Durations of Effusive Activity at Etna During the Period 1970 to 2010 Broken Out by Decade[a]

Decade	Number of Effusive Eruptions	Frequency (Eruptions per Year)	Volume ($\times 10^6$ m^3)	MOR ($m^3\ s^{-1}$)	Effusion (days)	Percent Time in Effusion
1970	30	3	182	0.6	1108	30
1980	15	1.5	258	0.8	642	18
1990	10	1	222	0.7	824	23
2000	13	1.3	299	0.9	1133	31
1970–2010	68	1.7	960	0.8	3707	25

[a]From data given in Appendix A.

voluminous flank eruptions and a high number of events from the newly formed SE Crater. Volumetrically, our data show that 542×10^6 m^3 of the 779×10^6 m^3 of lava erupted between 1980 and 2010 (or 70% of the total lava erupted) was associated with flank activity. It is worth noting that this figure does not change if we take into account also the volumes erupted by short-lived fire fountain events (Appendix B). In addition, 21 of the 38 (55%) of the effusive events listed in Table 2 were focused on the SE Crater, with all nine events since 2003 being centered on the SE Crater. *Behncke and Neri* [2003b] also point to the incidence of more frequent and more voluminous summit and flank eruptions since 1950, and remark that [*Behncke and Neri*, 2003b, p. 475] "if this trend continues, the activity of Etna might become similar to that of the 17th Century." We can confirm that this is indeed the case, and the 17th century trend has now been in place for 40 years.

5. Conclusion

[37] If we consider the period 1971–2010, Etna experienced effusive activity on 3735 days, or 25% of the time (Table 5). Through this time there was variation in terms of the frequency and duration of effusive activity, but erupted volumes on a decadal scale were typically of the order of 300×10^6 m^3 to keep the mean output rate between 0.6 and 0.9 m^3 s^{-1}; thereby maintaining a typical rate of 0.8 m^3 s^{-1} (Table 5). This compares with the rate of 0.7 m^3 s^{-1} obtained by *Wadge and Guest* [1981] for the period 1971–1981, and 0.8 m^3 s^{-1} for the period 1610–1669.

[38] The 30 year long satellite-derived discharge rate data set allows us to define the decadal volumetric behavior of the system, as well as to detail the volumetric trends and character of individual eruptions. This shows that, although the decadal-scale output remained stable between 1980 and 2010, the style with which this volume was erupted changed, with the 2001 eruption triggering a change in style: in 2001 eruption durations, syneruption volumetric trends, peak discharge rates and mean output rates all changed, as did the relation between discharge rate and flow area. Thus, although trends in long-term output appear stable and resilient, events such as that of 2001 can modify the manner in which this persistent flux is erupted. This suggests that the output rate is controlled by supply from the deep system, and cannot be changed by processes occurring in the shallow system; shallow system processes just serve to modify the way in which the flux is erupted. Thus, to change Etna's output rate, some profound change must occur in the deep system. Examining the cumulative output trends for the last 4 centuries show that such changes occurred in 1669 and 1971.

[39] We can conclude that Etna has displayed a remarkably steady output rate at least during the last 40 years. Similar steady state behavior, consistent with a constant flux of magma into and out of a crustal reservoir connected to the surface by an open conduit, has been detected at other volcanoes such as Stromboli [*Bertagnini et al.*, 2003; *Armienti et al.*, 2007; *Calvari et al.*, 2011] and Montserrat's Soufriére Hills [*Ryan et al.*, 2010; *Wadge et al.*, 2010], and for shorter periods at Kilauea [*Mattox et al.*, 1993] and Shishaldin [*Petersen and McNutt*, 2007]. This points to the resilience of output at such persistently active effusive (and extrusive) systems. Given that Etna is characterized by such steady supply and output rates we can propose that, unless the supply from deep system changes then, in the next decade, another 300×10^6 m^3 of lava will be erupted onto Etna's flanks. Uncertainty arises, however, in projecting how superficial effects, such as flank spreading, will serve to determine the way in which this volume is distributed across the decade. Will it be erupted in a small number of longer, lower TADR events (as during 1983–1993), or will it be erupted in a larger number of shorter, higher TADR events (as during 2000–2010)? If the output trend of the volcano remains similar to that observed post-2001, we can expect short-duration effusive phases with high discharge rates. The key question is, though, when will this current phase of high output end, and how will that end be marked?

Appendix A

[40] Volumes, durations and mean output rates for effusive activity at Etna during the period 1970–2010 can be collated using the published data listed at the end of this appendix, plus the data generated by us using the satellite data. The resulting collation is given in Table A1. The types of eruptive event included in this collation are discussed in Appendix B, where we note that volumes erupted during explosive events are not included. Nor do we include the short-lived fountaining events that occurred between 1996 and 2001, although the events grouped within the 1990 eruption tabulated in Table A1 are actually four short fountaining events (as broken out in Table 2) lasting 0.375 h, 0.46 h, 0.375 h and 0.2 h.

Appendix B

[41] Satellite-derived volumetric data presented in this paper cover a large proportion of the effusive products emplaced by Etna's eruptions during the past 30 years. These include almost all voluminous flank and summit effusive eruptions lasting more than 6 days. Appendix A lists 20 effusive events lasting greater than 6 days between 1980 and 2010, of which we have satellite data for 17. Just three are missing due to gaps in the data archive or cloud problems, these being the 10 day long eruption of September-October 1989 SE crater and E flank eruption, and the January-June 2000 eruption. We use volumetric measurements from the literature to fill in these missing volumes; we also use literature-derived volumes to fill in the data for effusive events lasting less than 6 days (as given in Appendix A).

[42] We find that the long-duration (greater than 6 days long) events account for 95 percent of the total volume erupted by effusive events (i.e., 737×10^6 m^3 of the 775×10^6 m^3 of lava erupted). Of this, 86 percent (666.5×10^6 m^3) has been captured by our satellite data sets. Our analysis considers the volumetric nature of these large volume effusive events.

[43] Two types of eruptive event are not covered in the Appendix A listing, and thus in our analysis: (1) voluminous tephra emission over extended periods (as occurred during the effusive eruptions of 2001 and 2002–2003) and (2) short-lived episodes of lava fountaining that erupt lava and tephra at high intensity, but over relatively short time periods (typically just a few hours in duration), as occurred between 1996 and 2001.

[44] While the volume of tephra emitted during each of these event types cannot be quantified using the methods

Table A1. Volumes, Durations, and Mean Output Rates for Effusive Activity at Etna During the Period 1970–2010[a]

Eruption	Start Date (dd-mm-yy)	Stop Date (dd-mm-yy)	Duration (days)	Volume ($\times 10^6$ m^3)	Cumulative ($\times 10^6$ m^3)	MOR (m^3 s^{-1})	Source[b]
1971	05-04-71	12-06-71	69	50	50	8.4	1
1971	01-06-71	01-09-71	93	7	57	0.9	1
1973	01-10-73	31-10-73	31	10	67	3.7	1
1974	31-01-74	17-03-74	46	6	73	1.5	1
1974	29-09-74	24-02-75	149	7	80	0.5	1
1975	24-02-75	12-09-75	201	13	93	0.7	1
1975	12-09-75	28-11-75	78	5	98	0.7	1
1975	29-11-75	17-06-76	202	12	110	0.7	1
1976	20-08-76	08-01-77	142	6	116	0.5	1
1977	16-07-77	22-07-77	7	1	117	1.7	1
1977	05-08-77	06-08-77	2	1	118	5.8	1
1977	14-08-77	14-08-77	1	4	122	46.3	1
1977	24-08-77	24-08-77	1	0.5	123	5.8	1
1977	02- 11-77	04-11-77	3	1	124	3.9	1
1977	07-11-77	08-11-77	2	1	125	5.8	1
1977	22-11-77	22-11-77	1	1	126	11.6	1
1977	25-11-77	25-11-77	1	1	127	11.6	1
1977	06-12-77	06-12-77	1	2	129	23.1	1
1977	10-12-77	13-12-77	4	0.5	129	1.4	1
1977	18-12-77	18-12-77	1	1	130	11.6	1
1977	24-12-77	25-12-77	2	1	131	5.8	1
1977	29-12-77	29-12-77	1	1	132	11.6	1
1978	02-01-78	04-01-78	3	2.5	135	9.6	1
1978	05-01-78	05-01-78	1	0.5	135	5.8	1
1978	07-01-78	07-01-78	1	0.5	136	5.8	1
1978	25-03-78	28-03-78	4	3	139	8.7	1
1978	29-04-78	05-06-78	38	23	162	7.0	1
1978	23-08-78	30-08-78	8	3	165	4.3	1
1978	23-11-78	30-11-78	8	5	170	7.2	1
1979	03-08-79	09-08-79	7	12	182	19.8	1
1980	01-09-80	01-09-80	30	4	186	127.3	1
1980	06-09-80	06-09-80	0.4	4.4	190	90.3	2
1980	26-09-80	26-09-80	0.5	3.9	194	61.7	2
1980	05-02-81	07-02-81	0.3	1.6	195	17.4	2
1981	17-03-81	23-03-81	2	3	198	28.9	2
1981	28-03-83	06-08-83	4.96	12.4	211	5.5	2
1983	27-04-84	16-10-84	131	62	273	1.3	2
1984	08-03-85	11-03-85	172	19	292	4.8	2
1985	12-03-85	13-07-85	1.2	0.5	292	1.4	2
1985	25-12-85	31-12-85	124	15	307	2.3	2
1985	14-09-86	24-09-86	6	1.2	309	0.5	2
1986	30-10-86	27-02-87	10	0.4	309	7.9	2
1986	11-09-89	27-09-89	120	82	391	0.5	2
1989	27-09-89	09-10-89	17	0.8	392	50.5	2
1989	04-01-90	02-02-90	11	48	440	23.0	2
1990	14-12-91	30-03-93	1.41	2.8	443	4.5	2
1991	21-07-96	19-08-96	471	183	626	0.2	3
1996	31-05-98	31-05-98	29	0.5	626	11.6	4
1998	22-07-98	22-07-98	1	1	627	34.7	5
1998	29-12-98	29-12-98	1	3	630	31.3	5
1998	04-02-99	24-08-99	1	2.7	633	0.7	5
1999	27-08-99	17-09-99	202	12	645	1.0	6
1999	17-10-99	05-11-99	22	1.9	647	8.1	6
1999	04-09-99	14-11-99	20	14	661	0.2	7
1999	26-01-00	24-06-00	72	1.1	662	1.5	6
2000	21-01-01	17-07-01	151	20	682	1.1	8
2001	17-07-01	09-08-01	177	17	699	19.1	9
2001	27-10-02	29-01-03	23	38	737	6.2	9
2002	07-09-04	08-03-05	94	50	787	4.1	9
2004	14-07-06	24-07-06	182	64	851	2.3	9
2006	12-10-06	14-12-06	10	2	853	6.8	9
2006	29-03-07	29-03-07	63	37	890	5.8	9
2007	11-04-07	11-04-07	1	0.5	890	5.8	9
2007	29-04-07	29-04-07	1	0.5	891	5.8	9
2007	06-05-07	6-05-07	1	0.5	891	5.8	9
2007	04-09-07	05-09-07	1	0.5	892	2.9	9
2007	13-05-08	07-07-09	2	0.5	892	1.9	9
2008	01-09-80	01-09-80	420	68	960	127.3	9

[a]See Appendix B for notes. Note that the events grouped within the 1990 eruption are actually four short events (as broken out in Table 2) lasting 0.375 h, 0.46 h, 0.375 h, and 0.2 h.

[b]Sources are numbered as follows: 1, *Wadge and Guest* [1981]; 2, unpublished measurements by J. B. Murray given by *Harris et al.* [2000]; 3, *Stevens et al.* [1997]; 4, *Andronico and Lodato* [2005]; 5, *Allard et al.* [2006]; 6, *Calvari et al.* [2003]; 7, *Harris and Neri* [2002]; 8, *Alparone et al.* [2003]; 9, integration of TADR data (this study).

applied here, lava fountaining episodes are too brief to be captured by the satellites that this study relies on.

[45] To check the underestimate in total erupted volume from not considering these events, we collated available literature data for them. These give the following additional volumes emplaced during tephra emissions and lava fountaining between 1996 and 2010: (1) Erupted volume during 105 fountain events spanning 1996–2001 was 90×10^6 m^3 (of which 72×10^6 m^3 was lava) [*Behncke et al.*, 2006]. (2) Erupted volume of pyroclastics during the July-August 2001 eruption was $5–10 \times 10^6$ m^3 [*Behncke and Neri*, 2003b]. (3) Erupted volume of pyroclastics during 2002–2003 was $4.4 \pm 0.6 \times 10^{10}$ kg (converts to $16.3 \pm 0.2 \times 10^6$ m^3 dense rock equivalent using a rock density of 2700 kg m^{-3}) [*Andronico et al.*, 2008a]. (4) Erupted volume during the 4–5 September 2007 SEC Crater fountain event was $2–4 \times 10^6$ m^3 (clastogenic lava flow) + $3.9–4.9 \times 10^5$ m^3 = $2.4–4.5 \times 10^6$ m^3 [*Andronico et al.*, 2008b].

[46] For the period 1980–2010, inclusion of these volumes adds 1.17×10^8 m^3 to the total of 7.75×10^8 m^3, meaning that the Appendix A collation of volumes associated with the main effusive events includes around 87 percent of the total erupted volume (8.92×10^8 m^3) during the three decades.

[47] For the period 2001–2010, inclusion of these volumes adds 2.73×10^7 m^3 to the total of 2.76×10^8 m^3 that we estimate was erupted during major summit and flank effusive events during this period (as given in Table 4), for a total erupted volume of 3.03×10^8 m^3. Thus, around 90% of the total erupted volume over this period was recorded by our satellite-based data and was partitioned into flank or summit lava flow fields. Addition of these "missing" volumes increases the time mean output over this 9 year period from 0.97 m^3 s^{-1} to 1.07 m^3 s^{-1}, thereby strengthening the trends, and conclusions, that we draw from our effused lava volume data set.

[48] **Acknowledgments.** We thank the three reviewers for their encouraging comments and helpful suggestions, as well as all University of Hawaii students who helped with AVHRR data processing, including John Bailey (1999 and 2001 data), Nicole Lautze (2001 data), and Lucas Moxey (2002–2003 data). All other data were processed by A.H. (pre-2000 data) and A.S. (post-2003 data). This contribution is in support of the LMV-based (PI: Franck Donnadieu) TerMex-MYSTRALS project "Contribution à l'évaluation des risques associés aux activités éruptives majeures de l'Etna: approche multidisciplinaire des processus et précurseurs." The AVHRR data and processing support provided by the NERC-NEODAAS group at the Plymouth Marine Laboratory (Plymouth, UK; http://www.neodaas.ac.uk) made this work possible. Their continued work and collaboration are gratefully acknowledged.

References

Acocella, V., B. Behncke, M. Neri, and S. D'Amico (2003), Link between major flank slip and 2002–2003 eruption at Mt. Etna (Italy), *Geophys. Res. Lett.*, *30*(24), 2286, doi:10.1029/2003GL018642.

Allard, P. (1997), Endogenous magma degassing and storage at Mount Etna, *Geophys. Res. Lett.*, *24*(17), 2219–2222, doi:10.1029/97GL02101.

Allard, P., J. Carbonnelle, N. Métrich, H. Loyer, and P. Zettwoog (1994), Sulphur output and magma degassing budget of Stromboli volcano, *Nature*, *368*, 326–330, doi:10.1038/368326a0.

Allard, P., B. Behncke, S. D'Amico, M. Neri, and S. Gambino (2006), Mount Etna 1993–2005: Anatomy of an evolving eruptive cycle, *Earth Sci. Rev.*, *78*, 85–114, doi:10.1016/j.earscirev.2006.04.002.

Alparone, S., D. Andronico, L. Lodato, and T. Sgroi (2003), Relationship between tremor and volcanic activity during the Southeast Crater eruption on Mount Etna in early 2000, *J. Geophys. Res.*, *108*(B5), 2241, doi:10.1029/2002JB001866.

Andronico, D., and L. Lodato (2005), Effusive activity at Mount Etna volcano (Italy) during the 20th century: A contribution to volcanic hazard assessment, *Nat. Hazards*, *36*, 407–443.

Andronico, D., S. Scollo, S. Caruso, and A. Cristaldi (2008a), The 2002–03 Etna explosive activity: Tephra dispersal and features of the deposits, *J. Geophys. Res.*, *113*, B04209, doi:10.1029/2007JB005126.

Andronico, D., A. Cristaldi, and S. Scollo (2008b), The 4–5 September 2007 lava fountain at South-East Crater of Mt Etna, Italy, *J. Volcanol. Geotherm. Res.*, *173*, 325–328, doi:10.1016/j.jvolgeores.2008.02.004.

Armienti, P., L. Francalanci, and P. Landi (2007), Textural effects of steady state behaviour of the Stromboli feeding system, *J. Volcanol. Geotherm. Res.*, *160*, 86–98, doi:10.1016/j.jvolgeores.2006.05.004.

Bailey, J. E., A. J. L. Harris, J. Dehn, S. Calvari, and S. K. Rowland (2006), The changing morphology of an open lava channel on Mt. Etna, *Bull. Volcanol.*, *68*, 497–515, doi:10.1007/s00445-005-0025-6.

Barnes, W. L., T. S. Pagano, and V. V. Salomonson (1998), Prelaunch characteristics of the Moderate Resolution Imaging Spectroradiometer (MODIS) on EOS-AM1, *IEEE Trans. Geosci. Remote Sens.*, *36*(4), 1088–1100, doi:10.1109/36.700993.

Behncke, B., and M. Neri (2003a), Cycles and trends in the recent eruptive behaviour of Mount Etna (Italy), *Can. J. Earth Sci.*, *40*, 1405–1411, doi:10.1139/e03-052.

Behncke, B., and M. Neri (2003b), The July-August 2001 eruption of Mt. Etna (Sicily), *Bull. Volcanol.*, *65*, 461–476, doi:10.1007/s00445-003-0274-1.

Behncke, B., M. Neri, E. Pecora, and V. Zanon (2006), The exceptional activity and growth of the Southeast Crater, Mount Etna (Italy), between 1996 and 2001, *Bull. Volcanol.*, *69*, 149–173, doi:10.1007/s00445-006-0061-x.

Bertagnini, A., N. Métrich, P. Landi, and M. Rosi (2003), Stromboli volcano (Aeolian Archipelago, Italy): An open window on the deep-feeding system of a steady state basaltic volcano, *J. Geophys. Res.*, *108*(B7), 2336, doi:10.1029/2002JB002146.

Branca, S., and P. Del Carlo (2004), Eruptions of Mt. Etna during the past 3,200 years: A revised compilation integrating the historical and stratigraphic records, in *Mt. Etna: Volcano Laboratory*, *Geophys. Monogr. Ser.*, vol. 143, edited by A. Bonaccorso et al., pp. 1–27, AGU, Washington, D. C.

Brown, J. W., O. B. Brown, and R. H. Evans (1993), Calibration of Advanced Very High Resolution Radiometer infrared channels: A new approach to nonlinear correction, *J. Geophys. Res.*, *98*(C10), 18,257–18,268, doi:10.1029/93JC01638.

Burton, M., et al. (2005), Etna 2004–05: An archetype for geodynamically controlled effusive eruptions, *Geophys. Res. Lett.*, *32*, L09303, doi:10.1029/2005GL022527.

Calvari, S., and the Whole Scientific Staff of INGV-Sezione di Catania (2001), Multidisciplinary approach yields insight into Mt. Etna 2001 eruption, *Eos Trans. AGU*, *82*(52), 653–656, doi:10.1029/01EO00376.

Calvari, S., M. Coltelli, M. Neri, M. Pompilio, and V. Scribano (1994), The 1991–93 Etna eruption: Chronology and lava flow field evolution, *Acta Vulcanol.*, *4*, 1–14.

Calvari, S., M. Neri, and H. Pinkerton (2003), Effusion rate estimations during the 1999 summit eruption on Mt. Etna, and growth of two distinct lava flow fields, *J. Volcanol. Geotherm. Res.*, *119*, 107–123, doi:10.1016/S0377-0273(02)00308-6.

Calvari, S., L. Spampinato, A. Bonaccorso, C. Oppenheimer, E. Rivalta, and E. Boschi (2011), Lava effusion—A slow fuse for paroxysms at Stromboli volcano?, *Earth Planet. Sci. Lett.*, *301*, 317–323, doi:10.1016/j.epsl.2010.11.015.

Clocchiatti, R., J. L. Joron, and M. Treuil (1988), The role of selective alkali contamination in the evolution of recent historic lavas of Mt. Etna, *J. Volcanol. Geotherm. Res.*, *34*, 241–249, doi:10.1016/0377-0273(88)90036-4.

Clocchiatti, R., M. Condomines, N. Guénot, and J. C. Tanguy (2004), Magma changes at Mount Etna: The 2001 and 2002–2003 eruptions, *Earth Planet. Sci. Lett.*, *226*, 397–414, doi:10.1016/j.epsl.2004.07.039.

Coltelli, M., C. Proietti, S. Branca, M. Marsella, D. Andronico, and L. Lodato (2007), Analysis of the 2001 lava flow eruption of Mt. Etna from three-dimensional mapping, *J. Geophys. Res.*, *112*, F02029, doi:10.1029/2006JF000598.

Condomines, M., J. C. Tanguy, and V. Michaud (1995), Magma dynamics at Mount Etna: Constraints from U-Th-Ra-Pb radioactive disequilibria and Sr isotopes in historical lavas, *Earth Planet. Sci. Lett.*, *132*, 25–41, doi:10.1016/0012-821X(95)00052-E.

Corsaro, R. A., R. Cristofolini, and L. Patané (1996), The 1669 eruption at Mount Etna: Chronology, petrology and geochemistry, with inferences on the magma sources and ascent mechanisms, *Bull. Volcanol.*, *58*, 348–358, doi:10.1007/s004450050144.

Corsaro, R. A., L. Miraglia, and M. Pompilio (2007), Petrologic evidence of a complex plumbing system feeding the July-August 2001 eruption of Mt. Etna, Sicily, Italy, *Bull. Volcanol.*, *69*, 401–421, doi:10.1007/s00445-006-0083-4.

Cracknell, A. P. (1997), *The Advanced Very High Resolution Radiometer*, 534 pp., Taylor and Francis, London.

Crisci, G. M., S. Di Gregorio, R. Rongo, M. Scarpelli, W. Spataro, and S. Calvari (2003), Revisiting the 1669 Etnean eruptive crisis using a cellular automata model and implications for volcanic hazard in the Catania area, *J. Volcanol. Geotherm. Res.*, *123*, 211–230, doi:10.1016/S0377-0273(03)00037-4.

Favalli, M., A. Fornaciai, F. Mazzarini, A. J. L. Harris, M. Neri, B. Behncke, M. T. Pareschi, S. Tarquini, and E. Boschi (2010), Evolution of an active lava flow field using a multitemporal LIDAR acquisition, *J. Geophys. Res.*, *115*, B11203, doi:10.1029/2010JB007463.

Frazzetta, G., and R. Romano (1984), The 1983 Etna eruption: Event chronology and morphological evolution of the lava flow, *Bull. Volcanol.*, *47*, 1079–1096, doi:10.1007/BF01952364.

Guest, J. E. (1973), The summit of Mt. Etna prior to the 1971 eruptions, *Philos. Trans. R. Soc. London*, *274*(1238), 63–78, doi:10.1098/rsta.1973.0026.

Guest, J. E., and A. M. Duncan (1981), Internal plumbing of Mount Etna, *Nature*, *290*, 584–586, doi:10.1038/290584a0.

Harris, A. J. L. (1996), Low spatial resolution thermal monitoring of volcanoes from space, Ph.D. thesis, Open Univ., Milton Keynes, U. K.

Harris, A. J. L., and S. M. Baloga (2009), Lava discharge rates from satellite-measured heat flux, *Geophys. Res. Lett.*, *36*, L19302, doi:10.1029/2009GL039717.

Harris, A. J. L., and M. Neri (2002), Volumetric observations during paroxysmal eruptions at Mount Etna: Pressurized drainage of a shallow chamber or pulsed supply?, *J. Volcanol. Geotherm. Res.*, *116*, 79–95, doi:10.1016/S0377-0273(02)00212-3.

Harris, A. J. L., S. Blake, D. A. Rothery, and N. F. Stevens (1997), A chronology of the 1991 to 1993 Mount Etna eruption using advanced very high resolution radiometer data: Implications for real-time thermal volcano monitoring, *J. Geophys. Res.*, *102*(B4), 7985–8003, doi:10.1029/96JB03388.

Harris, A. J. L., J. B. Murray, S. E. Aries, M. A. Davies, L. P. Flynn, M. J. Wooster, R. Wright, and D. A. Rothery (2000), Effusion rate trends at Etna and Krafla and their implications for eruptive mechanisms, *J. Volcanol. Geotherm. Res.*, *102*, 237–269, doi:10.1016/S0377-0273(00)00190-6.

Harris, A. J. L., J. Dehn, and S. Calvari (2007), Lava effusion rate definition and measurement: A review, *Bull. Volcanol.*, *70*, 1–22, doi:10.1007/s00445-007-0120-y.

Harris, A. J. L., M. Favalli, A. Steffke, A. Fornaciai, and E. Boschi (2010), A relation between lava discharge rate, thermal insulation, and flow area set using lidar data, *Geophys. Res. Lett.*, *37*, L20308, doi:10.1029/2010GL044683.

Hughes, J. W., J. E. Guest, and A. M. Duncan (1990), Changing styles of effusive eruption on Mount Etna since AD 1600, in *Magma Transport and Storage*, edited by M. P. Ryan, pp. 385–405, John Wiley, New York.

James, M. R., H. Pinkerton, and M. Ripepe (2010), Imaging short period variations in lava flux, *Bull. Volcanol.*, *72*, 671–676, doi:10.1007/s00445-010-0354-y.

Kidwell, K. B. (1995), NOAA polar orbiter data users guide (TIROS-N, NOAA-6, NOAA-7, NOAA-8, NOAA-9, NOAA-10, NOAA-11, NOAA-12, NOAA-13, and NOAA-14), NOAA, Washington, D. C.

Lautze, N. C., A. J. L. Harris, J. E. Bailey, M. Ripepe, S. Calvari, J. Dehn, S. Rowland, and K. Evans-Jones (2004), Pulsed lava effusion at Mount Etna during 2001, *J. Volcanol. Geotherm. Res.*, *137*, 231–246, doi:10.1016/j.jvolgeores.2004.05.018.

Mattox, T. N., C. Heliker, J. Kauahikaua, and K. Hon (1993), Development of the 1990 Kalapana Flow Field, Kilauea Volcano, Hawaii, *Bull. Volcanol.*, *55*, 407–413, doi:10.1007/BF00302000.

Métrich, N., P. Allard, N. Spilliaert, D. Andronico, and M. Burton (2004), 2001 flank eruption of the alkali- and volatile-rich primitive basalt responsible for Mount Etna's evolution in the last three decades, *Earth Planet. Sci. Lett.*, *228*, 1–17, doi:10.1016/j.epsl.2004.09.036.

Neri, M., and V. Acocella (2006), The 2004–2005 Etna eruption: Implications for flank deformation and structural behaviour of the volcano, *J. Volcanol. Geotherm. Res.*, *158*, 195–206, doi:10.1016/j.jvolgeores.2006.04.022.

Neri, M., V. Acocella, B. Behncke, V. Maiolino, A. Ursino, and R. Velardita (2005), Contrasting triggering mechanisms of the 2001 and 2002–2003 eruptions of Mount Etna (Italy), *J. Volcanol. Geotherm. Res.*, *144*, 235–255, doi:10.1016/j.jvolgeores.2004.11.025.

Petersen, T., and S. McNutt (2007), Seismo-acoustic signals associated with degassing explosions recorded at Shishaldin Volcano, Alaska, 2003–2004, *Bull. Volcanol.*, *69*, 527–536, doi:10.1007/s00445-006-0088-z.

Pieri, D. C., and S. M. Baloga (1986), Eruption rate, area, and length relationships for some Hawaiian lava flows, *J. Volcanol. Geotherm. Res.*, *30*, 29–45, doi:10.1016/0377-0273(86)90066-1.

Rothery, D. A., M. Coltelli, D. Pirie, M. J. Wooster, and R. Wright (2001), Documenting surface magmatic activity at Mount Etna using ATSR remote sensing, *Bull. Volcanol.*, *63*, 387–397, doi:10.1007/s004450100153.

Rowland, S. K., A. J. L. Harris, M. J. Wooster, F. Amelung, H. Garbeil, L. Wilson, and P. J. Mouginis-Mark (2003), Volumetric characteristics of lava flows from interferometric radar and multispectral satellite data, *Bull. Volcanol.*, *65*(5), 311–330, doi:10.1007/s00445-002-0262-x.

Ruch, J., V. Acocella, F. Storti, M. Neri, S. Pepe, G. Solaro, and E. Sansosti (2010), Detachment depth revealed by rollover deformation: An integrated approach at Mount Etna, *Geophys. Res. Lett.*, *37*, L16304, doi:10.1029/2010GL044131.

Ryan, G., S. C. Loughlin, M. R. James, E. S. Calder, T. Christopher, M. H. Strutt, and G. Wadge (2010), Growth of the lava dome and extrusion rates at Soufrière Hills Volcano, Montserrat, West Indies: 2005–2008, *Geophys. Res. Lett.*, *37*, L00E08, doi:10.1029/2009GL041477.

Salomonson, V. V., W. L. Barnes, P. W. Maymon, H. E. Montgomery, and H. Ostrow (1989), MODIS: Advanced facility instrument for studies of the Earth as a system, *IEEE Trans. Geosci. Remote Sens.*, *27*(2), 145–153, doi:10.1109/36.20292.

Solaro, G., V. Acocella, S. Pepe, J. Ruch, M. Neri, and E. Sansosti (2010), Anatomy of an unstable volcano from InSAR: Multiple processes affecting flank instability at Mt. Etna, 1994–2008, *J. Geophys. Res.*, *115*, B10405, doi:10.1029/2009JB000820.

Spampinato, L., S. Calvari, C. Oppenheimer, and L. Lodato (2008), Shallow magma transport for the 2002–03 Mt. Etna eruption inferred from thermal infrared surveys, *J. Volcanol. Geotherm. Res.*, *177*, 301–312, doi:10.1016/j.jvolgeores.2008.05.013.

Steffke, A. M., A. J. L. Harris, M. Burton, T. Caltabiano, and G. G. Salerno (2011), Coupled use of COSPEC and satellite measurements to define the volumetric balance during effusive eruptions at Etna, Italy, *J. Volcanol. Geotherm. Res.*, *205*, 47–53, doi:10.1016/j.jvolgeores.2010.06.004.

Stevens, N. F., J. B. Murray, and G. Wadge (1997), The volume and shape of the 1991–1993 lava flow field at Mount Etna, Sicily, *Bull. Volcanol.*, *58*, 449–454, doi:10.1007/s004450050153.

Tanguy, J. C. (1980), L'Etna: Étude pétrologique et paléomagnetique: Implications volcanologiques, Ph.D. thesis, 618 pp., Univ. of Paris, Paris.

Vicari, A., A. Ciraudo, C. Del Negro, A. Herault, and L. Fortuna (2009), Lava flow simulations using discharge rates from thermal infrared satellite imagery during the 2006 Etna eruption, *Nat. Hazards*, *50*, 539–550, doi:10.1007/s11069-008-9306-7.

Wadge, G. (1981), The variation of magma discharge during basaltic eruptions, *J. Volcanol. Geotherm. Res.*, *11*, 139–168, doi:10.1016/0377-0273(81)90020-2.

Wadge, G., and J. E. Guest (1981), Steady-state magma discharge at Etna 1971–81, *Nature*, *294*, 548–550, doi:10.1038/294548a0.

Wadge, G., G. P. L. Walker, and J. E. Guest (1975), The output of the Etna volcano, *Nature*, *255*, 385–387, doi:10.1038/255385a0.

Wadge, G., R. Herd, G. Ryan, E. S. Calder, and J.-C. Komorowski (2010), Lava production at Soufrière Hills Volcano, Montserrat: 1995–2009, *Geophys. Res. Lett.*, *37*, L00E03, doi:10.1029/2009GL041466.

Weinreb, M. P., G. Hamilton, S. Brown, and R. J. Koczor (1990), Nonlinearity corrections in calibration of Advanced Very High Resolution Radiometer infrared channels, *J. Geophys. Res.*, *95*(C5), 7381–7388, doi:10.1029/JC095iC05p07381.

Wright, R., S. Blake, A. J. L. Harris, and D. A. Rothery (2001), A simple explanation for the space-based calculation of lava eruption rates, *Earth Planet. Sci. Lett.*, *192*, 223–233, doi:10.1016/S0012-821X(01)00443-5.

S. Calvari and L. Spampinato, Istituto Nazionale di Geofisica e Vulcanologia, Sezione di Catania, Piazza Roma 2, I-95123 Catania, Italy.

A. Harris, Laboratoire Magmas et Volcans, Université Blaise Pascal, 5 Rue Kessler, F-63038 Clermont-Ferrand, France. (a.harris@opgc.univ-bpclermont.fr)

A. Steffke, HIGP, SOEST, University of Hawai'i at Mānoa, 1680 East-West Rd., Honolulu, HI 96822, USA.